Enhanced Light Emission of Micro LEDs Using Graphene-Connected Micropillar Structures and Ag/SiO<inf>2</inf> Nanoparticles

ACS Photonics

Open Access

pubs.acs.org/journal/apchd5

Article

Enhanced Light Emission of Micro LEDs Using Graphene-Connected Micropillar Structures and Ag/SiO_2 Nanoparticles

Aoqi Fang, Qingqing Li, Jixin Liu, Zaifa Du,* Penghao Tang, Hao Xu, Yiyang Xie, Jibin Song, Kaixin Zhang, Tianxi Yang, Qun Yan, Weiling Guo,* and Jie Sun*

Cite This: https://doi.org/10.1021/acsphotonics.4c01514

Read Online

ACCESS | Metrics & More | Article Recommendations | Supporting Information

ABSTRACT: This paper reports on a micropillar micro-light-emitting diode (MP-μLED) enhanced by a graphene conductive layer and SiO_2-coated Ag nanoparticles (Ag/SiO_2 NPs). The micropillar structure enables direct contact between Ag/SiO_2 NPs and the quantum well (QW), leveraging localized surface plasmon resonance (LSPR) to enhance the emission of QW. The SiO_2 coating on Ag serves as an insulating layer, preventing energy leakage through electron tunneling between QW−Ag and Ag−Ag interfaces. Graphene, used as a transparent conductive layer, integrates the individual micropillars into a cohesive structure, ensuring efficient current spreading and uniform light emission. Compared to plane μLEDs of the same mesa size, the MP-μLED with graphene transparent electrodes and LSPR enhancement shows an improvement of 44% in external quantum efficiency (EQE) and 45% in wall plug efficiency (WPE) at a current density of 1000 A/cm^2. This study demonstrates the significant application potential of LSPR and micropillar structures in μLED technology.

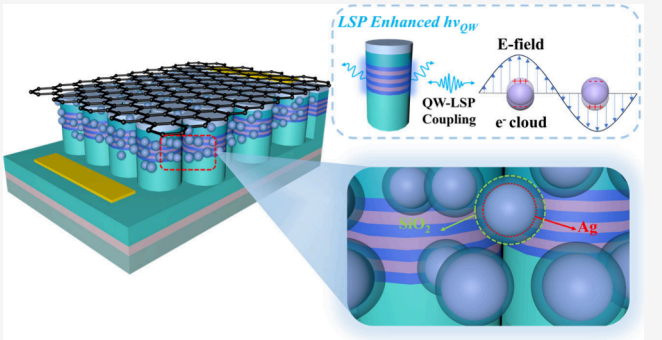

KEYWORDS: *localized surface plasmon resonance, graphene, micropillar, micro-LED*

INTRODUCTION

In the preparation method of full-color micro-LED (μLED) display arrays, blue μLEDs can serve as one of the three primary colors and integrate with green and red μLEDs to form a full-color display array.[1−3] Alternatively, blue μLEDs can be used as excitation light sources to excite green and red quantum dots to create a full-color display array.[4−10] Therefore, blue μLEDs are the core components in new display technologies, and their performance significantly affects the overall display effect of μLED full-color display arrays. However, due to material properties and sidewall defects, there is still significant room for improvement in the luminous efficiency and external quantum efficiency (EQE) of μLEDs.[11−14]

For GaN-based μLEDs, the significant difference between the refractive index of GaN (∼2.5) and that of air (∼1) results in a small light escape angle, limiting the light extraction efficiency (LEE).[15,16] Furthermore, in InGaN/GaN quantum wells (QW), the quantum-confined Stark effect (QCSE) primarily caused by piezoelectric polarization leads to a decrease in radiative recombination within the QWs.[17] In addition to material constraints, the impact of sidewall defects in μLEDs is also significant. This is because the sidewall area constitutes a large proportion of the emitting surface, and sidewall defects introduced during etching substantially increase the probability of nonradiative recombination in μLEDs, limiting the improvement of internal quantum efficiency (IQE).[18−21]

Localized surface plasmon resonance (LSPR) has been widely demonstrated to enhance the radiative recombination efficiency of LEDs.[22−24] However, LSPR strongly depends on the distance between the localized surface plasmon (LSP) and the QW, and significant coupling occurs only when this distance is less than 100 nm.[25,26] Micropillar (MP) structures can enable direct contact between the LSP and the QW with minimal sacrifice of the active region area, overcoming the distance limitation for LSP-QW coupling efficiency.[27] Moreover, MP structures can relieve stress, suppress QCSE, and provide more escape paths for photons, especially in GaN-based LEDs.[28,29]

In blue LEDs, Ag nanoparticles (NPs) are commonly used as LSPs. However, direct contact between the QW and Ag NPs can lead to electron tunneling between the QW and Ag NPs, resulting in energy annihilation. The same electron tunneling can occur between Ag NPs when they are in contact with each

Received: August 12, 2024
Revised: January 25, 2025
Accepted: January 28, 2025

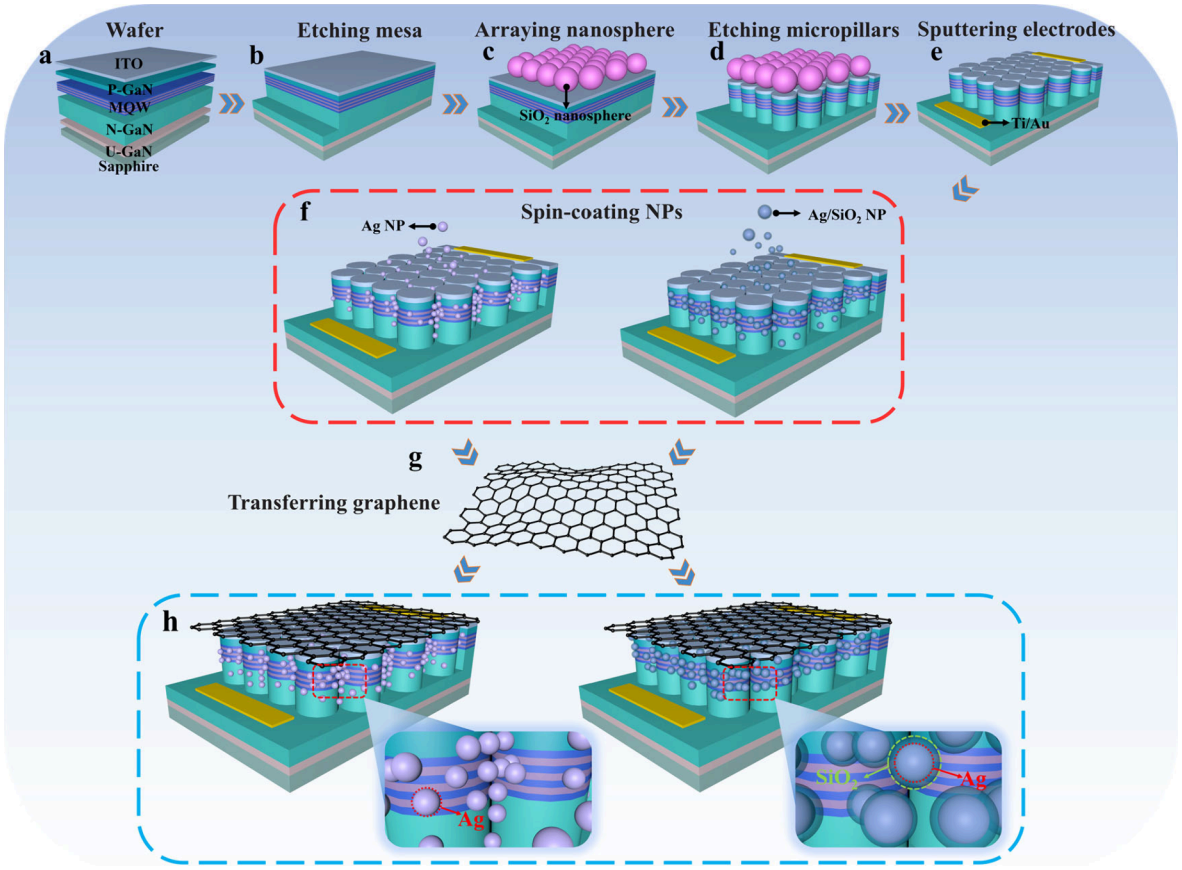

Figure 1. (a) Epitaxial structure; (b) Etching the light-emitting mesa; (c) Arranging SiO_2 nanospheres; (d). Etching micropillars; (e) Sputtering metal electrodes; (f) Spin-coating Ag NPs and Ag/SiO_2 NPs; (g) Transferring graphene; (h) Final device schematic.

other.[30−34] If there is an insulating layer on the surface of Ag NPs, the probability of such electron tunneling can be significantly reduced.[35,36] This insulating layer can also prevent the decrease in LSP coupling efficiency caused by the oxidation of Ag NPs.

To address the issues mentioned above, we etched micropillar arrays on the surface of μLEDs down to the N-GaN layer, exposing more QWs to the air. On this basis, Ag NPs with a SiO_2 insulating layer were filled into the gaps of the micropillar arrays, allowing direct contact between Ag/SiO_2 NPs and QWs. This approach utilizes LSPR to enhance the radiative recombination efficiency of carriers in the QWs. With the addition of Ag NPs wrapped in a SiO_2 insulating layer, the photoluminescence (PL) intensity of the micropillar arrays increased by 57%, compared to 19% when Ag NPs without the SiO_2 insulating layer were used. Considering issues related to current spreading and emission uniformity after etching the micropillars, we transferred a mono layer of graphene onto the surface of the micropillars as a transparent conductive layer. This layer connects the isolated micropillars, resulting in the fabrication of a micropillar-μLED (MP-μLED) that utilizes LSPR to enhance emission. This device demonstrated excellent optoelectronic performance. Compared to plane μLEDs of the same size, the MP-μLEDs with Ag/SiO_2 NPs exhibited a 45% increase in wall plug efficiency (WPE) and a 44% increase in EQE at a current density of 1000 A/cm^2.

MATERIALS AND METHODS

Figure 1 shows the fabrication method of LSPR enhanced MP-μLED. In this experiment, commercially available sapphire substrate GaN-based blue LED epitaxial wafers were used. To ensure good ohmic contact between the metal electrode and the P-GaN and to enhance current spreading, a 110 nm layer of indium tin oxide (ITO) was sputtered on the surface of the P-GaN as a current spreading layer. After this, inductively coupled plasma reactive ion etching (ICP-RIE) was used to etch the light-emitting mesa with dimensions of 50 μm × 50 μm. Subsequently, a dip-coating machine was used to cover the surface with 800 nm diameter SiO_2 nanospheres as an etching hard mask, and ICP-RIE was used to etch the micropillars. After removing the nanospheres, the sample was subjected to a KOH solution at 85 °C to repair sidewall damage incurred during the etching process. Subsequently, 300 nm of SiO_2 was deposited using inductively coupled plasma chemical vapor deposition (ICPCVD) as a sidewall passivation layer and electrode isolation layer. Then, 15/300 nm of Ti/Au was sputtered as the metal electrode. To investigate whether the presence of an insulating layer on the surface of Ag NPs has a significant impact on the performance of MP-μLEDs, Ag NPs and Ag/SiO_2 NPs were respectively spin-coated into the gaps of the micropillars to form control groups. After spin coating, the tops of the micropillars were gently wiped with a cotton swab to keep the micropillar surfaces clean. Finally, a monolayer layer of graphene was transferred as a transparent electrode to connect the micropillars, ensuring excellent emission uniformity and current spreading.

RESULTS

In this experiment, Ag NPs serve as the LSP, and the presence or absence of a SiO_2 insulating layer on the surface of the Ag

https://doi.org/10.1021/acsphotonics.4c01514
ACS Photonics XXXX, XXX, XXX−XXX

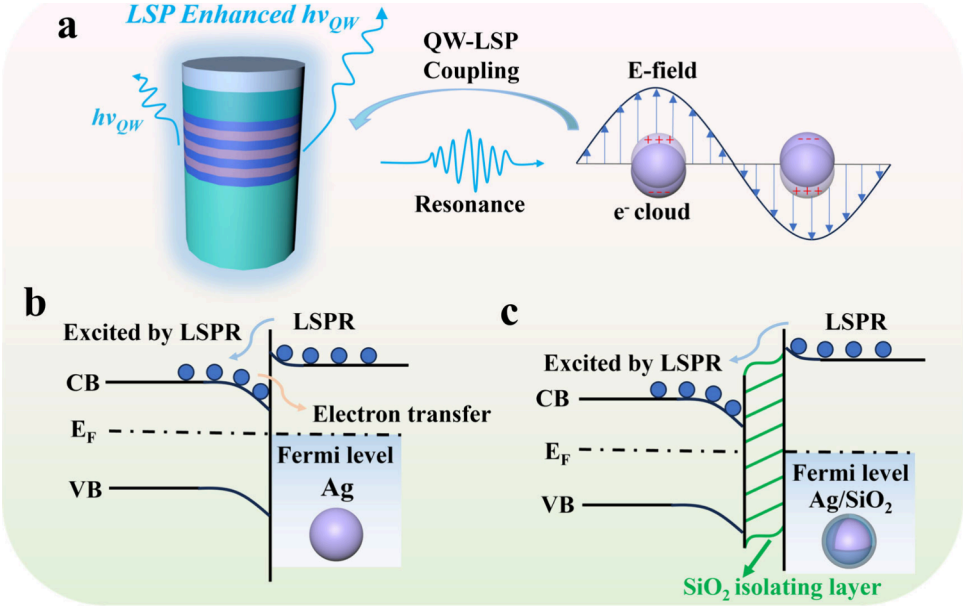

Figure 2. (a) QW-LSP coupling schematic; (b) Energy band structure when QW is in contact with Ag; (c) Energy band structure when QW is in contact with Ag/SiO_2.

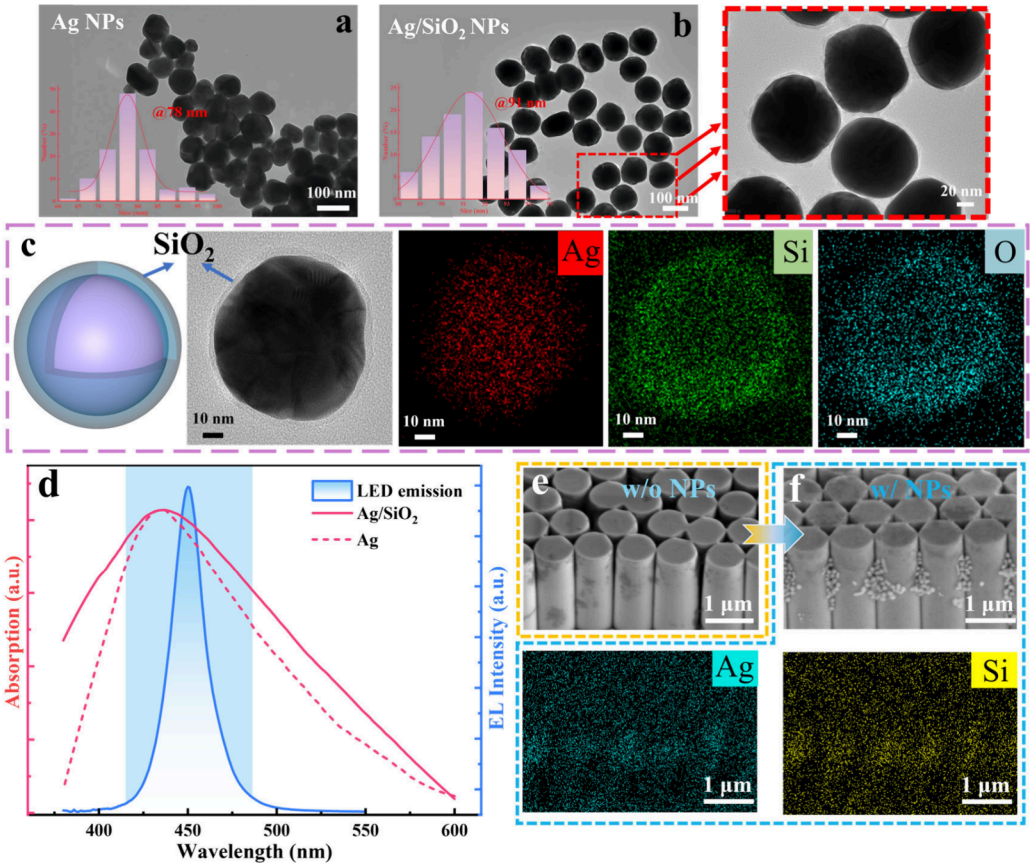

Figure 3. (a). TEM image of Ag NPs; (b) TEM image of Ag/SiO_2 NPs and enlarged view of the area marked with a red dashed line; (c) Structural schematic, TEM image, and corresponding EDS spectrum of a single Ag/SiO_2 NP; (d) Absorption spectra of Ag NPs and Ag/SiO_2 NPs; (e) Micropillar morphology before spin-coating NPs; (f) Micropillar morphology after spin-coating Ag/SiO_2 NPs and the corresponding EDS spectrum.

NPs is the variable under study. In the Supporting Information, we conducted experimental tests and simulation on Ag/SiO_2 with different thicknesses of SiO_2, ultimately setting the thickness of SiO_2 in this experiment at 5 nm.

Explanation of LSPR Mechanism and Charge Transfer between the QW and Ag. As shown in Figure 2a, the coupling mechanism of Ag NPs and QWs is based on LSPR. When the absorption wavelength of Ag NPs matches the

https://doi.org/10.1021/acsphotonics.4c01514
ACS Photonics XXXX, XXX, XXX−XXX

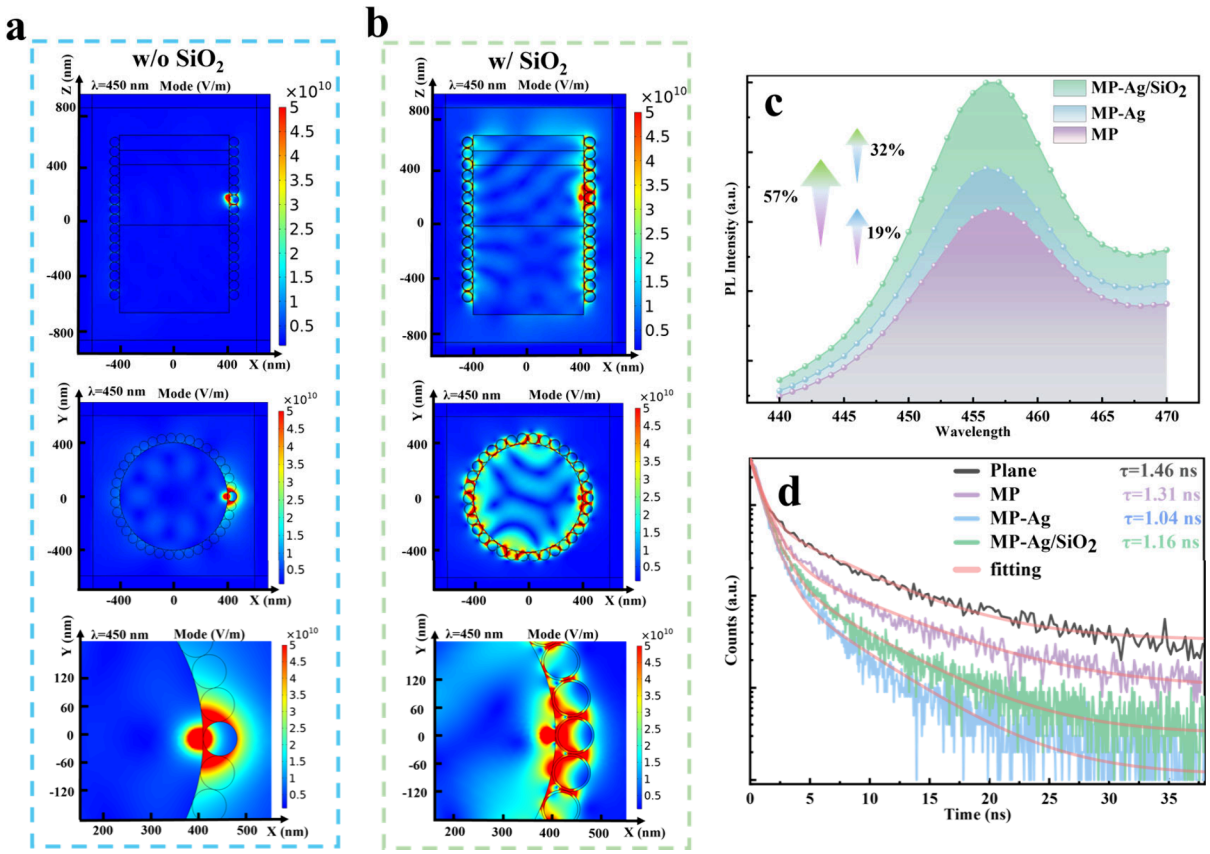

Figure 4. (a) Simulation results of Ag NPs with QWs; (b) Simulation results of Ag/SiO_2 NPs with QWs; (c) PL spectra of the three types of micropillars structures; (d) TRPL spectra of plane structure and micropillar structures.

emission wavelength of the QWs, LSPR occurs, enhancing the electromagnetic field near the QWs. This increases the radiative recombination efficiency of carriers in the QWs, thus enhancing the light output.

When the QW is in direct contact with or in very close proximity to Ag, another accompanying mechanism may occur; there can be charge transfer between the two. Figure 2b and c, respectively, illustrate the energy band diagrams when the QWs are in contact with Ag and Ag/SiO_2. The work function of QWs ranges from 4.5 to 5.5 eV, while that of Ag ranges from 4.26 to 4.74 eV. Electrons in the Ag can be excited to energy states above the conduction band edge of the QWs by surface plasmon waves. These excited electrons can then drop into the conduction band and defect levels of the QWs, increasing bandgap and defect emissions.[30] When the work function of the QWs is less than that of Ag, the energy band on the QW side bends upward, preventing electrons within the QWs from moving into the Ag and thus avoiding energy annihilation. However, when the work function of the QWs is greater than that of Ag, as shown in Figure 2b, The downward bending of the energy band on the QW side causes electrons to tunnel into the Ag, leading to energy annihilation. Adding an insulating layer between the Ag and QWs, as shown in Figure 2c, prevents the direct transfer of electrons from the QWs to the Ag, thus avoiding the energy annihilation caused by electron tunneling between the QWs and Ag. Based on this concept, our experiment investigated the differences in the effects of Ag/SiO_2 NPs and Ag NPs in enhancing the light-emission of MP-μLEDs.

NPs and MPs. We prepared Ag NPs without an insulating layer and Ag/SiO_2 NPs with SiO_2 insulating layers of 5 and 15 nm thicknesses, respectively. The detailed preparation process is provided in the supple information. Since the coupling efficiency of LSP with QW is highly dependent on their distance, we hypothesized that different thicknesses of SiO_2 would affect the experimental results. Therefore, we performed finite element analysis on the coupling of these three types of Ag NPs with QWs. The simulation results showed that the coupling was most effective when the SiO_2 thickness was 5 nm. To verify this simulation result, we incorporated these three types of Ag NPs into MP-μLEDs and measured their optical performance. We found that the devices with 5 nm SiO_2 exhibited the highest light output power and EQE, consistent with the simulation results. Therefore, we chose Ag/SiO_2 NPs with a 5 nm SiO_2 thickness for this study. The model construction and optical properties from the finite element analysis are presented in the Supporting Information.

Figure 3a and b are transmission electron microscope (TEM) images of Ag NPs without and with SiO_2 coating, respectively, showing relatively uniform spherical particles. Through the enlarged image at the red dashed line position, it can be seen that there is a layer of SiO_2 separating the NPs. The structural schematic and energy dispersive spectrometer (EDS) spectra of Ag/SiO_2 NPs are shown in Figure 3c, clearly indicating that the Ag/SiO_2 NPs are uniformly coated with SiO_2. This coating forms an insulating layer between Ag and QWs, preventing electron tunneling. As shown in Figure 3d, we measured the visible light absorption of Ag NPs and Ag/SiO_2 NPs, and both absorption spectra peaks matched the

https://doi.org/10.1021/acsphotonics.4c01514
ACS Photonics XXXX, XXX, XXX−XXX

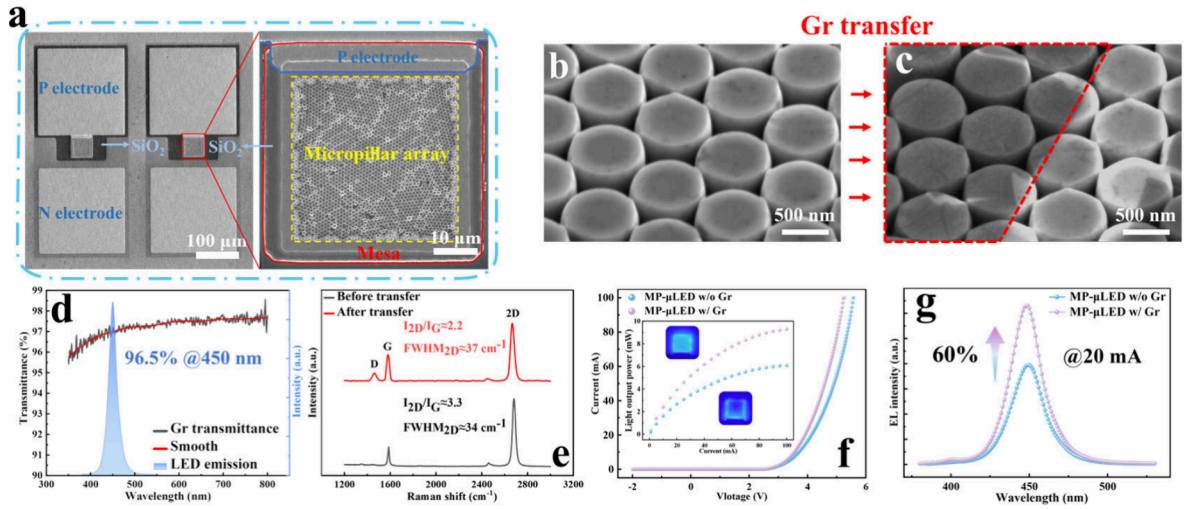

Figure 5. (a) Overall morphology of MP-μLED and the emitting surface morphology; (b, c) Surface morphology of micropillars before and after transferring graphene; (d) Transmittance of the graphene used in the experiment at different wavelengths; (e) Raman spectra before and after transferring graphene; (f) IV characteristics and light output power of MP-μLED before and after transferring graphene; (g) EL spectra of MP-μLED at 20 mA before and after transferring graphene.

emission spectrum range of the μLEDs prepared in this experiment. This match is one of the prerequisites for LSP resonance between Ag NPs and QWs. Another prerequisite is that the distance between Ag NPs and QWs should be less than 100 nm, which the micropillar structure can achieve. Figure 3e,f show the surface morphology of the etched micropillars and the surface morphology after spin-coating Ag/SiO_2 NPs, along with their EDS spectrum. It is evident that enough nanoparticles can be accommodated in the gaps of the micropillars. Therefore, with the help of the micropillar structure, the nanoparticles can be in close contact with the QWs, ensuring sufficient LSP coupling.

Figure 4a shows the finite element analysis structure of the coupling between Ag NPs and Ag/SiO_2 NPs with QWs. The detailed model construction is provided in the Supporting Information. In the absence of a SiO_2 insulating layer, the strong electric field is only distributed near the dipole positions and does not propagate throughout all LSPs in the system, which is likely caused by energy leakage due to electron tunneling during the direct contact between Ag-QW and Ag−Ag. This means that the energy generated by LSPR is only concentrated near the point dipole and cannot be effectively transferred throughout the structure. In contrast, Figure 4b shows a much more pronounced coupling effect between Ag/SiO_2 NPs and QWs. Each NP exhibits a strong LSPR, not just localized near the point dipole, indicating that the LSPR energy can be effectively transferred rather than being annihilated through electron tunneling.

The photoluminescence (PL) spectra of micropillars without any NPs, and those filled with Ag NPs and Ag/SiO_2 NPs, are shown in Figure 4c. The enhancement of the micropillar PL is more significant with the SiO_2-insulated Ag/SiO_2 NPs, increasing by 57%, whereas the enhancement is 19% without the SiO_2 insulating layer. Figure 4d shows the time-resolved photoluminescence (TRPL) spectra of the three samples and a plane structure. After etching the micropillars, the PL decay lifetime decreases due to improved epitaxial stress and reduced QCSE effect, leading to faster recombination of carriers in the QWs. When NPs are spin-coated on the micropillars, LSPs create an additional recombination channel with a very high density of photonic states, competing with nonradiative recombination channels and effectively increasing the IQE, thereby reducing the PL decay lifetime.[29]

It is noteworthy that MP-Ag exhibits the shortest PL decay lifetime, because without the SiO_2 insulating layer, the distance between Ag NPs and QWs is smaller. Since the coupling efficiency of LSP with QWs strongly depends on their distance, the coupling efficiency between Ag NPs and QWs is higher compared to Ag/SiO_2 NPs, resulting in a shorter PL decay lifetime. However, during the coupling process between Ag NPs and QWs, a large number of electrons tunnel from QWs to Ag, causing only a portion of the electrons generated by LSPR to enhance carrier radiative recombination and light output, while the rest are converted to nonradiative losses rather than enhanced exciton output. This energy loss partially quenches the PL intensity. This explains why MP-Ag has a faster PL decay lifetime but lower PL intensity compared to MP-Ag/SiO_2.

Graphene. Figure 5a is the scanning electron microscope (SEM) images of the MP-μLED and light-emitting mesa we fabricated. The light-emitting mesa size is 50 μm × 50 μm, and the micropillar area size is 40 μm × 40 μm. It can be seen that the micropillars are uniformly arranged and the gaps between the micropillars are sufficient to accommodate a large number of NPs. To enhance the current spreading of the MP-μLED, we transferred a monolayer graphene as a transparent conductive layer to connect the individual micropillars. Figure 5b and c show the surface morphology of the micropillars before and after transferring the graphene. Figure 5d shows the transmittance of the monolayer graphene used in this experiment at different wavelengths. In the emission wavelength range of the LED designed in this experiment, the transmittance reaches 96.5%. Figure 5e shows the Raman spectra of the graphene before and after transfer. The ratio of the 2D peak to the G peak and the full width at half-maximum (fwhm) of the 2D peak indicate that this is a monolayer graphene.

The optoelectronic properties before and after transferring the graphene are shown in Figure 5f,g. Without the graphene, the MP-μLED's micropillar area emits weakly. After trans-

https://doi.org/10.1021/acsphotonics.4c01514
ACS Photonics XXXX, XXX, XXX−XXX

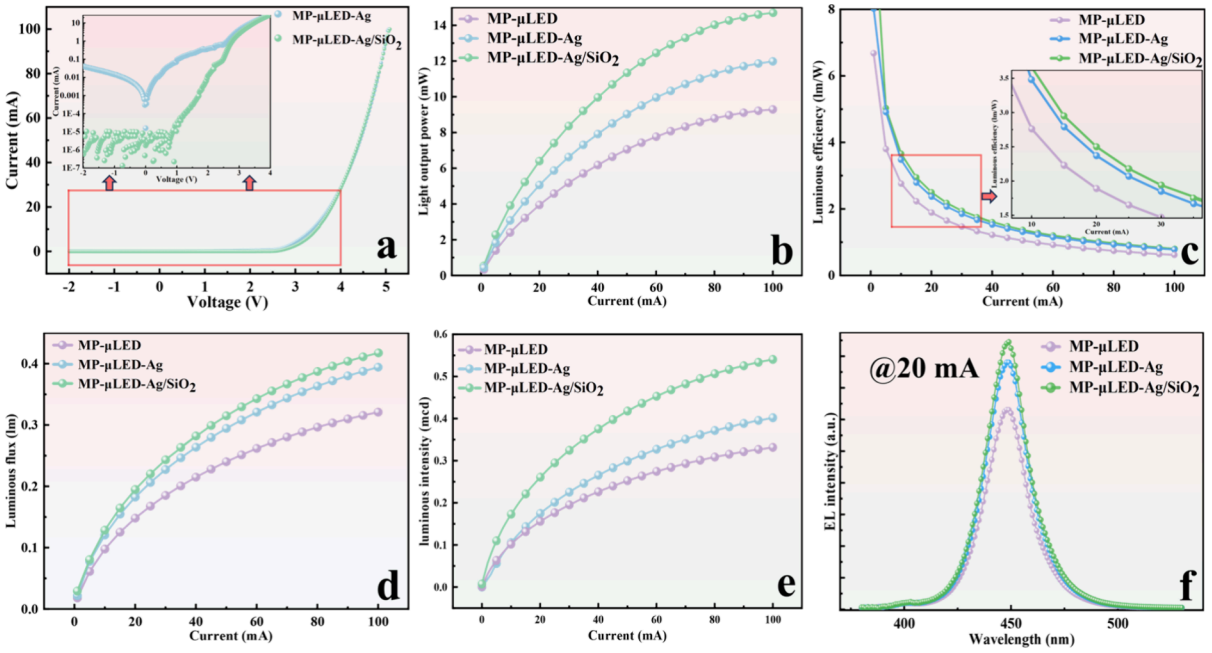

Figure 6. (a) *I*−*V* characteristics of the two types of MP-μLEDs with NPs. Optical performance of MP-μLEDs without NPs, with Ag NPs, and with Ag/SiO_2 NPs: (b) light output power, (c) luminous efficiency, (e) luminous flux, (d) luminous intensity, and (f) EL spectra at 20 mA.

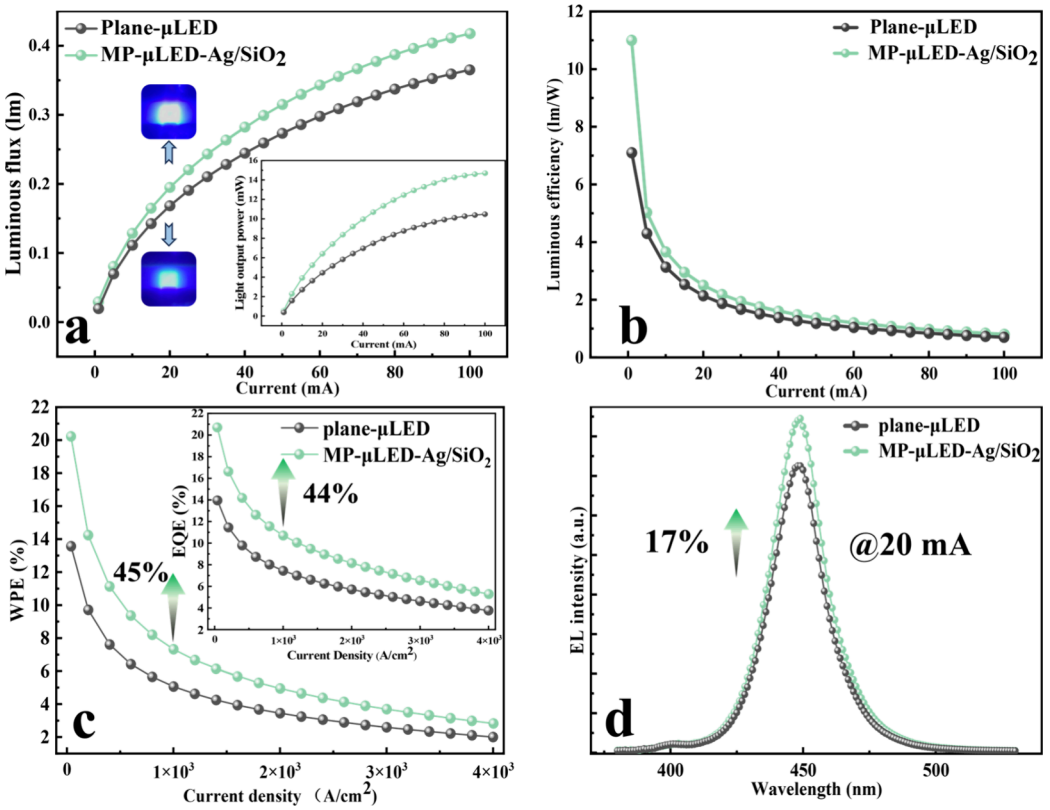

Figure 7. Comparison of optical performance between MP-μLEDs with Ag/SiO_2 NPs and plane μLEDs: (a) luminous flux and light output power, (b) luminous efficiency, (c) WPE and EQE, and (d) EL spectra at 20 mA.

ferring the graphene, the emission becomes more uniform, and the micropillar area can light up normally, significantly improving the light output power. The electroluminescence (EL) intensity of the MP-μLED after transferring graphene increased by 60% at a current of 20 mA, and the turn-on resistance was also lower. This indicates that using graphene as a transparent conductive layer to connect the micropillars is feasible.

Comparison of Different Devices. We tested the electrical and optical properties of the three types of MP-μLEDs after transferring graphene. Figure 6a shows the *I*−*V* characteristics of the two MP-μLEDs with nanoparticles. The

https://doi.org/10.1021/acsphotonics.4c01514
ACS Photonics XXXX, XXX, XXX−XXX

MP-μLED with Ag NPs exhibits approximately 0.5 mA of leakage current, which might be due to the short circuit between P-GaN and N-GaN caused by the aggregation of Ag NPs in the micropillar gaps. In contrast, the MP-μLED with Ag/SiO_2 NPs shows almost no leakage current because the SiO_2 insulating layer prevents this issue, highlighting one of the advantages of Ag/SiO_2 NPs. Figure 6b−f, respectively, show the light output power, luminous efficiency, luminous flux, luminous intensity, and EL spectra at a current of 20 mA for the three types of MP-μLEDs. The MP-μLED with Ag/SiO_2 NPs demonstrates the best optical performance, further confirming the effectiveness of using Ag/SiO_2 NPs with an insulating layer to enhance the emission of MP-μLEDs.

We compared the MP-μLEDs with Ag/SiO_2 to plane μLEDs of the same size. Figure 7a shows the comparison of the two devices in terms of luminous flux with the light output power presented as the inset. The comparison of luminous efficacy is shown in Figure 7b. The MP-μLED-Ag/SiO_2 consistently exhibited superior optical performance. The comparison of WPE and EQE is shown in Figure 7c, where the inset shows the EQE. at a current density of 1000 A/cm^2, the EQE and WPE increased by 44% and 45%, respectively. Figure 7d shows the EL spectra of the two devices under a driving current of 20 mA (800 A/cm^2). The EL intensity of MP-μLED-Ag/SiO_2 has increased by 17% compared with that of Plane-μLED. This comparison indicates that the proposed MP-μLEDs with Ag/SiO_2 NPs have the potential to outperform traditional plane μLEDs in practical applications, demonstrating superior performance.

DISCUSSION

In this paper, we present a μLED with a micropillar structure, where the micropillars are connected by a monolayer graphene transparent conductive layer, ensuring excellent current spreading and emission uniformity. Using a spin-coating method, we filled the gaps between the micropillars with Ag NPs and Ag/SiO_2 NPs, whose absorption resonance peaks match the emission wavelength of the μLED. The micropillar structure allows close contact between the QWs and Ag NPs, enhancing the optical performance of the μLED through LSPR. To investigate the impact of the SiO_2 insulating layer on the optical performance of MP-μLEDs, we conducted finite element analysis and device testing. We found that Ag/SiO_2 NPs with an insulating layer significantly improved the optical performance of MP-μLEDs, and thinner SiO_2 layers had a more pronounced effect on enhancing the device's optical performance. Compared to plane μLEDs, the MP-μLEDs with graphene transparent electrodes and LSP coupling showed a 44% increase in EQE and a 45% increase in WPE at a current density of 1000 A/cm^2. We believe this work paves the way for future practical applications of nanostructures and LSP in μLEDs, demonstrating a significant potential for improved performance.

ASSOCIATED CONTENT

Supporting Information

The Supporting Information is available free of charge at https://pubs.acs.org/doi/10.1021/acsphotonics.4c01514.

Preparation processes of Ag NPs and Ag/SiO_2 NPs; TEM images of Ag NPs and Ag/SiO_2 NPs with different SiO_2 layer thicknesses; Construction method and results of finite element analysis model for coupling of Ag NPs and Ag/SiO_2 NPs with QWs; Optical performance comparison of MP-μLED with Ag NPs and Ag/SiO_2 NPs of different SiO_2 layer thicknesses; The cross-sectional structure of MP-μLED and the schematic diagram of micropillar; The comparison of the electrical and optical performance of four types of devices: plane-μLED, MP-μLED, MP-μLED-Ag, and MP-μLED-Ag/SiO_2; The comparison of the electrical and optical performance of plane-μLED and MP-μLED; The TRPL spectra of the micropillar structures and their corresponding energy conversion efficiency (DOCX)

AUTHOR INFORMATION

Corresponding Authors

Zaifa Du − *School of Physics and Electronic Information, Weifang University, Weifang 261061, China;* orcid.org/0000-0002-4269-5504; Email: dzfwfu@wfu.edu.cn

Weiling Guo − *Key Laboratory of Optoelectronics Technology, Beijing University of Technology, Beijing 100124, China;* Email: guoweiling@bjut.edu.cn

Jie Sun − *Fujian Science and Technology Innovation Laboratory for Optoelectronic Information of China and College of Physics and Information Engineering, Fuzhou University, Fuzhou 350100, China; Quantum Device Physics Laboratory, Department of Microtechnology and Nanoscience, Chalmers University of Technology, Gothenburg 41296, Sweden;* orcid.org/0000-0002-6479-7771; Email: jie.sun@fzu.edu.cn

Authors

Aoqi Fang − *Key Laboratory of Optoelectronics Technology, Beijing University of Technology, Beijing 100124, China;* orcid.org/0009-0006-9297-9296

Qingqing Li − *New Cornerstone Science Laboratory, MOE Key Laboratory for Analytical Science of Food Safety and Biology, College of Chemistry, Fuzhou University, Fuzhou 350108, China*

Jixin Liu − *Key Laboratory of Optoelectronics Technology, Beijing University of Technology, Beijing 100124, China*

Penghao Tang − *Key Laboratory of Optoelectronics Technology, Beijing University of Technology, Beijing 100124, China*

Hao Xu − *Key Laboratory of Optoelectronics Technology, Beijing University of Technology, Beijing 100124, China*

Yiyang Xie − *Key Laboratory of Optoelectronics Technology, Beijing University of Technology, Beijing 100124, China;* orcid.org/0000-0001-8563-2004

Jibin Song − *State Key Laboratory of Chemical Resource Engineering, College of Chemistry, Beijing University of Chemical Technology, Beijing 10010, China;* orcid.org/0000-0003-4771-5006

Kaixin Zhang − *Fujian Science and Technology Innovation Laboratory for Optoelectronic Information of China and College of Physics and Information Engineering, Fuzhou University, Fuzhou 350100, China*

Tianxi Yang − *Fujian Science and Technology Innovation Laboratory for Optoelectronic Information of China and College of Physics and Information Engineering, Fuzhou University, Fuzhou 350100, China*

Qun Yan − *Fujian Science and Technology Innovation Laboratory for Optoelectronic Information of China and College of Physics and Information Engineering, Fuzhou University, Fuzhou 350100, China*

https://doi.org/10.1021/acsphotonics.4c01514
ACS Photonics XXXX, XXX, XXX−XXX

Complete contact information is available at:
https://pubs.acs.org/10.1021/acsphotonics.4c01514

Funding

This work was supported by National Key Research and Development Program of China (2023YFB3608703 and 2023YFB3608700), National Natural Science Foundation of China (12474066), Fujian Science and Technology Innovation Laboratory for Optoelectronic Information of China (2021ZZ122 and 2020ZZ110), Fujian Provincial Project (2021HZ0114 and 2024J011312), and Wuhan Municipal Project (2024010702020024).

Notes

The authors declare no competing financial interest.

REFERENCES

(1) Qi, L.; Li, P.; Zhang, X.; Wong, K. M.; Lau, K. M. Monolithic full-color active-matrix micro-LED micro-display using InGaN/AlGaInP heterogeneous integration. *Light Sci. Appl.* **2023**, *12* (1), 258.

(2) Shin, J.; Kim, H.; Sundaram, S.; Jeong, J.; Park, B.; Chang, C. S.; Choi, J.; Kim, T.; Saravanapavanantham, M.; Lu, K.; Kim, S.; Suh, J. M.; Kim, K. S.; Song, M.; Liu, Y.; Qiao, K.; Kim, J. H.; Kim, Y.; Kang, J.; Kim, J.; Lee, D.; Lee, J.; Kim, J. S.; Lee, H. E.; Yeon, H.; Kum, H.; Bae, S.; Bulovic, V.; Yu, K. J.; Lee, K.; Chung, K.; Hong, Y. J.; Ougazzaden, A.; Kim, J. Vertical full-colour micro-LEDs via 2D materials-based layer transfer. *Nature* **2023**, *614* (7946), 81−87.

(3) Li, L.; Tang, G.; Shi, Z.; Sheng, X.; et al. Transfer-printed, tandem microscale light-emitting diodes for full-color displays. *Proc. Natl. Acad. Sci. USA* **2021**, *118* (18), No. e2023436118.

(4) Xu, F.; Tao, T.; Zhang, D.; Zhang, Y.; Sang, Y.; Yu, J.; Zhi, T.; Zhuang, Z.; Xie, Z.; Zhang, R.; Liu, B. Wafer-Scale Monolithic Integration of Blue Micro-Light-Emitting Diodes and Green/Red Quantum Dots for Full-Color Displays. *IEEE Electron Device Lett.* **2023**, *44* (8), 1320−1323.

(5) Bae, J.; Shin, Y.; Yoo, H.; Choi, Y.; Lim, J.; Jeon, D.; Kim, I.; Han, M.; Lee, S. Quantum dot-integrated GaN light-emitting diodes with resolution beyond the retinal limit,". *Nat. Commun.* **2022**, *13* (1), 1862.

(6) Hwangbo, S.; Hu, L.; Hoang, A. T.; Choi, J. Y.; Ahn, J. Wafer-scale monolithic integration of full-colour micro-LED display using MoS2 transistor. *Nat. Nanotechnol.* **2022**, *17* (5), 500−506.

(7) Qi, L.; Zhang, X.; Chong, W. C.; Lau, K. M. Monolithically integrated high-resolution full-color GaN-on-Si micro-LED microdisplay. *Photon. Res.* **2023**, *11* (1), 109−120.

(8) Lee, T. Y.; Chen, L. Y.; Lo, Y. Y.; Swayamprabha, S. S.; Kumar, A.; Huang, Y. M.; Chen, S. C.; Zan, H. W.; Chen, F. C.; Horng, R. H.; Kuo, H. C. Technology and Applications of Micro-LEDs: Their Characteristics, Fabrication, Advancement, and Challenges. *ACS Photonics* **2022**, *9* (9), 2905−2930.

(9) Liang, K. L.; Kuo, W. H.; Shen, H. T.; Lin, S. F.; Fang, Y. H.; Lai, Y. Y.; Lin, C. C. Highly Efficient Fine-Pitch Quantum Dot/Titanium Oxide Nanocomposites for Ultrahigh-Resolution Full-Color Micro-Light Emitting Diode Displays. *ACS Photonics* **2024**, *11* (8), 2981−2991.

(10) Ma, T.; Chen, J.; Chen, Z.; Liang, L.; Hu, J.; Shen, J.; Li, Z.; Zeng, H. Progress in Color Conversion Technology for Micro-LED. *Advanced Materials Technologies* **2023**, *8* (1), 2200632.

(11) Gaurav, A.; Tsai, C. Y.; Wang, G. W.; Tsai, H. Y.; Ye, Z. T.; Lin, C. F. Ultrahigh-resolution full-color micro-LED array with enhanced efficiency based on a color conversion technique. *Photon. Res.* **2023**, *11* (6), 925−935.

(12) Olivier, F.; Daami, A.; Licitra, C.; Templier, F. Shockley-Read-Hall and Auger non-radiative recombination in GaN based LEDs: A size effect study. *Appl. Phys. Lett.* **2017**, *111* (2), 022104.

(13) Chen, P. W.; Hsiao, P. W.; Chen, H. J.; Lee, B. S.; Chang, K. P.; Yen, C. C.; Horng, R. H.; Wuu, D. S. On the mechanism of carrier recombination in downsized blue micro-LEDs. *Sci. Rep.* **2021**, *11* (1), 22788.

(14) Park, J. H.; Pristovsek, M.; Cai, W.; Tanaka, A.; Furusawa, Y.; Han, D. P.; Seong, T. Y.; Amano, H.; Cheong, H. Impact of Sidewall Conditions on Internal Quantum Efficiency and Light Extraction Efficiency of Micro-LEDs. *Adv. Opt. Mater.* **2023**, *11* (10), 2203128.

(15) Ke, M. Y.; Wang, C. Y.; Chen, L. Y.; Chen, H. H.; Chiang, H. L.; Cheng, Y. W.; Hsieh, M. Y.; Chen, C. P.; Huang, J. Application of Nanosphere Lithography to LED Surface Texturing and to the Fabrication of Nanorod LED Arrays. *IEEE J. Sel. Top. Quantum Electron.* **2009**, *15* (4), 1242−1249.

(16) Xu, K.; Xu, C.; Xie, Y.; Deng, J.; Zhu, Y.; Guo, W.; Mao, M.; Xun, M.; Chen, M.; Zheng, L.; Sun, J. GaN nanorod light emitting diodes with suspended graphene transparent electrodes grown by rapid chemical vapor deposition. *Appl. Phys. Lett.* **2013**, *103* (22), 222105.

(17) Ryou, J. H.; Yoder, P. D.; Liu, J.; Lochner, Z.; Kim, H.; Choi, S.; Kim, H. J.; Dupuis, R. D. Control of Quantum-Confined Stark Effect in InGaN-Based Quantum Wells. *IEEE J. Sel. Top. Quantum Electron.* **2009**, *15* (4), 1080−1091.

(18) Boussadi, Y.; Rochat, N.; Barnes, J. P.; Bakir, B. B.; Ferrandis, P.; Masenelli, B.; Licitra, C. Investigation of sidewall damage induced by reactive ion etching on AlGaInP MESA for micro-LED application. *J. Lumin.* **2021**, *234*, 117937.

(19) Smith, J. M.; Ley, R.; Wong, M. S.; Baek, Y. H.; Kang, J. H.; Kim, C. H.; Gordon, M. J.; Nakamura, S.; Speck, J. S.; DenBaars, S. P. Comparison of size-dependent characteristics of blue and green InGaN microLEDs down to 1 μm in diameter. *Appl. Phys. Lett.* **2020**, *116* (7), 071102.

(20) Hwang, D.; Mughal, A.; Pynn, C. D.; Nakamura, S.; DenBaars, S. P. Sustained high external quantum efficiency in ultrasmall blue III−nitride micro-LEDs. *Appl. Phys. Express* **2017**, *10* (3), 032101.

(21) Jin, Y. K.; Chiang, H. Y.; Lin, K. H.; Lee, C. A.; Huang, J. J. Luminescence efficiency improvement of small-size micro light-emitting diodes by a digital etching technology. *Opt. Lett.* **2022**, *47* (23), 6277−6280.

(22) Fadil, A.; Ou, Y.; Iida, D.; Kamiyama, S.; Petersen, P. M.; Ou, H. Combining surface plasmonic and light extraction enhancement on InGaN quantum-well light-emitters. *Nanoscale* **2016**, *8* (36), 16340.

(23) Du, Z.; Chen, E.; Feng, H.; Qian, F.; Xiong, F.; Tang, P.; Guo, W.; Song, J.; Yan, Q.; Guo, T.; Sun, J. Efficiency improvement of GaN-based micro-light-emitting diodes embedded with Ag NPs into a periodic arrangement of nano-hole channel structure by ultra close range localized surface plasmon coupling. *Nanotechnology* **2022**, *33* (49), 495202.

(24) Wang, X.; Tian, Z.; Zhang, M.; Li, Q.; Su, X.; Zhang, Y.; Hu, P.; Li, Y.; Yun, F. Enhanced coupling efficiency and electrical property in surface plasmon-enhanced light-emitting diodes with the tapered Ag structure. *Opt. Express* **2020**, *28* (24), 35708−35715.

(25) Lee, I. H.; Jang, L. W.; Polyakov, A. Y. Performance enhancement of GaN-based light emitting diodes by the interaction with localized surface plasmons. *Nano Energy* **2015**, *13*, 140−173.

(26) Kholmicheva, N.; Royo Romero, L.; Cassidy, J.; Zamkov, M. Prospects and applications of plasmon-exciton interactions in the near-field regime. *Nanophotonics* **2019**, *8* (4), 613−628.

(27) Du, Z.; Feng, H.; Liu, Y.; Tang, P.; Qian, F.; Sun, J.; Guo, W.; Song, J.; Chen, E.; Guo, T.; Yan, Q. Localized surface plasmon coupling nanorods with graphene as a transparent conductive electrode for micro light-emitting diodes. *IEEE Electron Device Lett.* **2022**, *43* (12), 2133−2136.

(28) Kim, H. M.; Cho, Y. H.; Lee, H.; Kim, S.; Ryu, S. R.; Kim, D. Y.; Kang, T. W.; Chung, K. S. High-brightness light emitting diodes using dislocation-free indium gallium nitride/gallium nitride multi-quantum-well nanorod arrays. *Nano Lett.* **2004**, *4* (6), 1059−1062.

(29) Pandey, A.; Min, J.; Reddeppa, M.; Malhotra, Y.; Xiao, Y.; Wu, Y.; Sun, K.; Mi, Z. An Ultrahigh Efficiency Excitonic Micro-LED. *Nano Lett.* **2023**, *23* (5), 1680−1687.

(30) Sigle, W.; Nelayah, J.; Koch, C. T.; van Aken, P. A. Electron energy losses in Ag nanoholes—from localized surface plasmon resonances to rings of fire. *Opt. Lett.* **2009**, *34* (14), 2150−2152.
(31) Jang, L. W.; Jeon, D. W.; Sahoo, T.; Polyakov, A. Y.; Saravanakumar, B.; Yu, Y. T.; Cho, Y. H.; Yang, J. K.; Lee, I. H. Energy coupling processes in InGaN/GaN nanopillar light emitting diodes embedded with Ag and Ag/SiO_2 nanoparticles. *J. Mater. Chem.* **2012**, *22* (40), 21749−21753.
(32) Jang, L. W.; Jeon, D. W.; Kim, M.; Jeon, J. W.; Polyakov, A. Y.; Ju, J. W.; Lee, S. J.; Baek, J. H.; Yang, J. K.; Lee, I. H. Investigation of Optical and Structural Stability of Localized Surface Plasmon Mediated Light-Emitting Diodes by Ag and Ag/SiO_2 Nanoparticles. *Adv. Funct. Mater.* **2012**, *22* (13), 2728−2734.
(33) Lin, H. Y.; Chen, Y. F.; Wu, J. G.; Wang, D. I.; Chen, C. C. Carrier transfer induced photoluminescence change in metal-semiconductor core-shell nanostructures. *Appl. Phys. Lett.* **2006**, *88* (16), 161911.
(34) Anger, P.; Bharadwaj, P.; Novotny, L. Enhancement and quenching of single-molecule fluorescence. *Phys. Rev. Lett.* **2006**, *96* (11), 113002.
(35) Jang, L. W.; Sahoo, T.; Jeon, D. W.; Kim, M.; Jeon, J. W.; Jo, D. S.; Kim, M. K.; Yu, Y. T.; Polyakov, A. Y.; Lee, I. H. Quantum efficiency control of InGaN/GaN multi-quantum-well structures using Ag/SiO_2 core-shell nanoparticles. *Appl. Phys. Lett.* **2011**, *99* (25), 251114.
(36) Kim, T.; Uthirakumar, P.; Cho, Y. H.; Lee, I. H. Enabling Localized Surface Plasmon Emission from InGaN/GaN Nano-LEDs Integrated with Ag/SiO_2 Nanoparticles. *ACS Photonics* **2024**, *11* (2), 570−579.

https://doi.org/10.1021/acsphotonics.4c01514
ACS Photonics XXXX, XXX, XXX−XXX